Non-coding RNA Research 7 (2022) 133–141

Contents lists available at ScienceDirect

Non-coding RNA Research

journal homepage: www.keaipublishing.com/en/journals/non-coding-rna-research

Original Research Article

miR-204-5p in vivo inhibition cause diminished CD45RO cells rate in lungs of melanoma B16-bearing mice

Nadezhda Palkina [a], Mariya Aksenenko [a], Danil Zemtsov [a], Semyon Lavrentev [a], Ivan Zinchenko [a], Vasiliy Belenyuk [c], Andrey Kirichenko [b], Andrey Savchenko [c], Tatiana Ruksha [a,*]

[a] Department of Pathophysiology, Krasnoyarsk State Medical University, Krasnoyarsk, 660022, Russia
[b] Department of Pathological Anatomy, Krasnoyarsk State Medical University, Krasnoyarsk, 660022, Russia
[c] Laboratory of Cell Molecular Physiology and Pathology, Federal Research Center, Krasnoyarsk Science Center of The Siberian Branch of The Russian Academy of Sciences, Krasnoyarsk, 660022, Russia

ARTICLE INFO

Keywords:
Apoptosis
CD45RO
Melanoma B16
miR-204-5p
miR-211
microRNA LNA inhibitor

ABSTRACT

The treatment of melanoma remains a challenge, despite novel approaches recently becoming available for disseminated tumors. RNA targeting is being intensively studied in various types of disease. The aim of the present study was to explore whether the in vivo use of a microRNA (miR)-204-5p inhibitor affected melanoma progression, and whether its metastasis affects target organ remodeling. $CD45RO^+$, $CD3^+$, $CD8^+$, forkhead box $P3^+$, smooth muscle α-$actin^+$ cells in the lungs of B16 melanoma-bearing mice were evaluated using immunohistochemistry following miR-204-5p inhibitor transfection. Next, CD45RO expression in peripheral blood mononuclear cells (PBMCs), as well as the apoptosis of these cells, were measured by flow cytometry. The results revealed that the number of $CD45RO^+$ cells was decreased in the lungs of B16 melanoma-bearing mice and $CD45RO^+$ PBMCs following the use of an miR-204-5p inhibitor, which was associated with increased levels of PBMC apoptosis. In conclusion, the findings of the present study suggested that targeting miR-204-5p in melanoma metastasis target organs could be used to develop novel approaches for the treatment of disseminated forms of the disease.

1. Introduction

Melanoma is a type of skin cancer with a high rate of cancer-associated deaths; however, treatment of melanoma has markedly improved within the last decade due to targeted and immunotherapy within clinical practice [1,2]. Thus, the rates of overall survival in patients with melanoma have markedly increased [3]. While metastasis plays a crucial role in patient outcome and therapeutic efficacy, the molecular mechanisms underlying the specific processes associated with melanoma require further elucidation.

Metastasis is a systemic process that is driven by numerous genetic and epigenetic factors, and involves a precise interaction between primary tumors and metastasis target organs, which begins at the pre-metastatic stage [4]. The target organs of metastasis provide a microenvironment that facilitates the progression of distant secondary tumors [5]. Becoming obvious that cancer cells are able to migrate and disseminate within various stages of primary tumors starting at early stages [6]. Notably, intercellular communication between primary tumors and distant organs is supported by exosomes that transport various molecules, such as proteins and non-coding RNAs, from primary tumors to parenchymal organs, thus stimulating their rearrangement [7,8].

MicroRNAs (miRNAs/miRs) are single-stranded small non-coding RNAs that act as post-transcriptional regulators of gene expression [9]. Since miRNAs are differentially expressed in different organs and their expression is altered during the development of pathological states, they are considered potential diagnostic markers and therapeutic targets. However, limitations such as poor intracellular uptake of miRNA mimics/inhibitors and their degradation by endonucleases, markedly hinder their therapeutic efficacy [10]. A locked nucleic acid (LNA) inhibitor specific to miR-122 has been shown to effectively inhibit

* Corresponding author.
E-mail addresses: MosmanNV@yandex.ru (N. Palkina), aksenenko_mariya@mail.ru (M. Aksenenko), danil_zemtsov@mail.ru (D. Zemtsov), SemyonLavrentev@mail.ru (S. Lavrentev), Zinchenko.Ivan.003@gmail.com (I. Zinchenko), dyh.88@mail.ru (V. Belenyuk), krasak.07@mail.ru (A. Kirichenko), aasavchenko@yandex.ru (A. Savchenko), tatyana_ruksha@mail.ru (T. Ruksha).

https://doi.org/10.1016/j.ncrna.2022.06.001
Received 12 March 2022; Received in revised form 31 May 2022; Accepted 1 June 2022
Available online 3 June 2022

hepatitis C virus replication in vivo [11]. Patisiran, whose action is based on RNA targeting, has been approved for the treatment of hereditary transthyretin-mediated amyloidosis treatment [12].

The miR-204 family consists of miR-204-5p and miR-211. It was previously found that miR-204-5p inhibition diminishes proliferation but stimulates melanoma metastasis in vitro [13]. Several other studies have demonstrated that miR-204-5p acts as a tumor suppressor to diminish tumor growth and metastasis formation in various cancer cell types [14–16]. Both of the aforementioned miRNAs were targeted using the BRAFV600E-specific inhibitor, vemurafenib, to determine their corresponding roles in melanoma. Notably, treatment with vemurafenib increased the expression levels of miR-204-5p in BRAFV600E-positive melanoma cells via phosphorylation of the STAT3 transcription factor. Moreover, miR-204-5p overexpression impaired the migration of melanoma cells. By contrast, miR-211 is controlled by the MITF transcription factor, and the pigmentation of melanoma cells was enhanced following treatment with vemurafenib. Notably, miR-211 overexpression diminished sensitivity to vemurafenib [17]. Previous research using a zebrafish melanoma model revealed that miR-204-5p favors BRAFV600E-driven melanoma development [18]. These findings indicate the potential role of miR-204-5p in melanomagenesis, and highlights miR-204-5p as a potential target for the treatment of melanoma.

Therefore, the present study aimed to further examine the effects of miR-204-5p by exposing B16 melanoma-bearing mice to a miR-204-5p LNA™ specific inhibitor (LNA-i-204-5p).

2. Materials and methods

2.1. Animals

C57Bl6 female mice (age, 8 weeks) were purchased from the Russian National Center for Genetic Resources of Laboratory Animals at the 'SPF-vivarium' of the Federal Research Center Institute of Cytology and Genetics, Siberian Branch of the Russian Academy of Sciences (Novosibirsk, Russia). Following a 2-week acclimatization period, mice with a weight of 16.83–21.13 g were used in the study. Mice had ad libitum access to food and water, and were maintained in a 12-h light/dark cycle at 22–25 °C. The study was approved by the Local Ethics Committee of the Krasnoyarsk State Medical University (approval no. 79/2017; date issued, November 22, 2017). Due to ethical concerns, sample sizes between study groups (in particular, the control and inhibition groups) were kept at low levels and were therefore unequal between groups. The number of animals used in the groups did not exceed the maximum recommended number for biomedical studies involving animals, and was not less than the minimum number required for comparison by nonparametric statistical methods.

2.2. Blood samples and peripheral blood mononuclear cell (PBMC) culture

PBMCs were obtained from 5 healthy volunteers by separating buffy coats at Ficoll-Paque gradients (Biolot, St. Petersburg, Russian Federation). Written informed consent was provided from the patients. PBMCs were cultured in RPMI-1640 medium (Thermo Fisher Scientific, Inc., Waltham, MA, USA) supplemented with 300 mg l-glutamine, antibiotic-antimycotic (Thermo Fisher Scientific, Inc.) and 10% fetal calf serum (Thermo Fisher Scientific, Inc.) in a CO_2-incubator (model no. MSO-5AC; Sanyo Electric Co. Ltd.) at 37 °C and 5% CO_2. All procedures were performed in accordance with the Declaration of Helsinki.

2.3. miR-204-5p inhibition in vivo

B16 melanoma cells were purchased from the American Type Culture Collection and defrosted for use in subsequent experiments. A cell suspension (1×10^6) was injected subcutaneously into the left lower flank of mice (0.5 ml/mouse). Next, 7 days after inoculation, when melanoma cells had formed a palpable tumor, the mice were randomized into three groups: i) The control group treated with sterile 0.01 M phosphate-buffered saline (PBS; Control; n = 3); ii) the negative control group transfected with Negative Control A miRCURY LNA™ (Qiagen AB, Sollentuna, Sweden; Negative Control; n = 6); and iii) the experimental group transfected with mmu-miR-204-5p miRCURY LNA™ (LNA-i-204-5p) (Qiagen AB; n = 5) weekly at a dose of 25 mg/kg of animal weight. LNA™ inhibitors are high-affinity analogs of RNA with a ribose ring modification, making these compounds more specific and highly stable. Thus, the optimal treatment protocol was determined based on the manufacturer's protocol, and our previous data [19]. Mice were administered the calculated amount of inhibitor by subcutaneous injection into the cervical fold once every 7 days, on days 7 and 14 following melanoma cell transplantation. On day 15, which corresponds to the end of the pre-metastatic period and the beginning of the metastatic period of transplanted melanoma [20], the animals were sacrificed.

2.4. miR-204-5p inhibition in vitro

When PBMCs had reached the final concentration of 1×10^5 cells/ml, transfection experiments were performed using 1.5 μl Lipofectamine® 3000 (Thermo Fisher Scientific, Inc.)/500 μl cell suspension. *Anti*-miR solutions containing DMEM culture medium supplemented (Paneco, Moscow, Russian Federation) were added to the cells at a final concentration of 25 nM. The medium was replaced 24 h after transfection. *Anti*-miR™ miRNA Inhibitor Negative Control #1 (5 nmol lyophilized pellets; Thermo Fisher Scientific, Inc.) was used as a control for the miR-204-5p *Anti*-miR® miRNA Inhibitor (Thermo Fisher Scientific, Inc.). The measurement of miR-204-5p expression is described below. This experiment was repeated three times.

2.5. Tumor growth inhibition and mouse activity study

Tumor size was measured once every 2 days. Tumor volume was calculated as follows: Tumor volume (mm^3) = (tumor length x tumor $width^2$) x 0.5. The growth inhibition index (%) was defined as: (Mean volume of treated tumor - mean volume of control tumor)/mean volume of control tumor x 100. At the end of the experiment, mice were euthanized, the tumors were harvested, and bodies weight, internal organs and tumor weights were evaluated. To estimate the effect of the LNA inhibitor on mouse activity as a marker of drug toxicity, the activity index was scored daily as follows: 0, death; 1, coma with lack of activity, immobility and without reaction to tactile stimuli; 2, minimal motor activity with active movements including weak, mostly involuntary reactions to tactile stimuli; 3, slow movement (animal moving a few steps only when pushed) with the reaction to tactile stimuli being 'avoidance'; 4, subnormal motor activity in the form of slow active movements along the cage, the reaction to tactile stimuli being 'avoidance-defensive with attempts to bite'; and 5, normal motor activity, active movement across the cage, with reaction to tactile stimuli being 'avoidance with pronounced defensive reactions'. The body weight of each mouse was measured at the beginning of the experiment, prior to B16 melanoma cell transplantation and once every 3 days.

2.6. Immunohistochemistry

Formalin-fixed paraffin-embedded tissue sections (4-μm thick) were immunostained with primary antibodies against CD45RO (dilution, 1:200), CD3 (dilution, 1:150), CD8 (dilution, 1:50), forkhead box P3 (FOXP3; dilution, 1:20) and smooth muscle α-actin (α-SMA; dilution, 1:800) (all from Thermo Fisher Scientific, Inc.). 3-Amino-9-ethylcarbazole was used as a chromogen. Negative controls were treated similarly but without the primary antibody. Positively stained cells were evaluated using an Olympus BX-41 microscope (Olympus Corporation,

Tokyo, Japan) with an Infinity 2 Lumenera camera (Lumenera Corporation, Ottawa, Canada) and analyzed using commercial Infinity Capture and Infinity Analyze software (version 6.5.2, Lumenera Corporation, Ottawa, Canada). The slides were viewed at a magnification of ×400, and 10 fields were randomly selected for further analysis of antigen expression. Positively stained cells were calculated in each of the 10 representative fields and averaged per group, and the mean cell count score per organ per animal was obtained.

2.7. RNA isolation and reverse transcription-quantitative PCR (RT-qPCR)

Total RNA was extracted from homogenized tissue samples or cultured PBMCs using diaGene RNA isolation kit for cells (Dia-m, Moscow, Russian Federation, https://www.dia-m.ru), according to the manufacturer's instructions, and then eluted with 50 μl nuclease-free water. The concentration of total RNA and miRNA was quantified using a Qubit® HS RNA Assay kit and Qubit® microRNA Assay kit (Invitrogen; Thermo Fisher Scientific, Inc.), respectively, on a Qubit® 2.0 instrument (Invitrogen; Thermo Fisher Scientific, Inc.). To estimate the efficiency of LNA-i-miR-204-5p transfection in mouse tumors and melanoma metastasis target organs, miR-204-5p expression was assessed in the tumor, and lungs and liver of the LNA-i-miR-204-5p mice, compared with Negative Control and Control mice. Reverse transcription reaction was performed using MMLV RT kit (Evrogen, Moscow, Russia). RT-qPCR was performed using a total of 3 μl RNA solution with 1.5 μl 5x RT primer from the corresponding microRNA kit (cat. no. 4427975; Applied Biosystems; Thermo Fisher Scientific, Inc.), and 1.5 μl of a random decanucleotide primer included in the MMLV RT kit was heated in a thermostat at 70 °C for 2 min and subsequently cooled on ice. A total of 5.5 μl of the reaction mixture was added to the sample, consisting of 1 μl dNTP-mix, 1 μl 1,4-dithiothreitol, 2 μl 5X-first standard buffer, 0.5 μl MMLV reverse transcriptase and 1 μl nuclease-free water. The mixture was subsequently incubated in a thermostat at 37 °C for 50 min, and the reaction was stopped by heating the samples for 10 min at 70 °C.

Amplification of the obtained cDNA was performed on a StepOne™ Real-Time PCR-System using 2 μl per sample (Applied Biosystems; Thermo Fisher Scientific, Inc.) with the following thermocycling conditions: 50 °C for 2 min; 95 °C for 10 min; and 40 cycles of 95 °C for 15 s and 60 °C for 1 min. The fluorescent signal of carboxy-X-rhodamine (ROX) was subsequently detected. The reaction mixture used to determine the expression of both miRNA and mRNA in a total volume of 18 μl consisted of 1 μl 20x specific primers, 8 μl 2.5-fold reaction mixture for RT-qPCR in the presence of ROX (Syntol, Moscow, Russian Federation, http://www.syntol.ru) and 9 μl nuclease-free water. The reaction was performed on a StepOne™ Real-Time PCR system (Thermo Fisher Scientific, Inc.). The relative expression of miRNA was calculated using the $2^{-\Delta\Delta Ct}$ method and is expressed as fold-change as was described previously [21]. The geometric mean of U6snRNA and SnoRNA234 (cat. nos. RT001973 and RT001234, respectively; Thermo Fisher Scientific, Inc.) was used as a control reference for miRNA target.

2.8. Flow cytometry for apoptosis and CD45RO expression detection

PBMCs from healthy volunteers were transfected with miR-204-5p or negative control and incubated in 24-well plates at 37 °C in 5% CO_2 for 48 h. The cells were stained using the Annexin V-FITC/7-Aminoactinomycin D (7-AAD) kit (cat. no. IM3614; Beckman Coulter, Inc., Quebec, Canada), according to the manufacturer's instructions. The proportion of viable (Annexin V^-/7-AAD^-), early apoptotic (Annexin V^+/7-AAD^-) and late apoptotic/necrotic (Annexin V^+/7-AAD^+) cells was detected with Cytomics FC-500 using a NAVIOS laser flow cytometer (both Beckman Coulter, Inc.) and Navios™ cytometer running Cytometry List Mode Data Acquisition and Analysis Software version 1.3 (all from Beckman Coulter, Inc.). The experiments were performed in triplicate. The percentage of CD45RO cells was assessed after staining with CD45RO-electron coupled dye (Beckman Coulter, Inc.). Annexin-V and 7-AAD staining was further analyzed on gated CD45RO cells, and the levels of apoptosis in CD45RO cells were calculated as a percentage of the Annexin-V^+/7-AAD^- CD45RO cells among the 7-AAD^- cells. This experiment was repeated three times.

2.9. Detection of inflammatory cytokines by ELISAs

The serum levels of inflammatory markers, including IL-1β, IL-6 and TNF-α, were detected using commercial mouse TNF-α (cat. no. BMS607-3; Invitrogen; Thermo Fisher Scientific, Inc.), IL-1α (BMS611; Invitrogen; Thermo Fisher Scientific, Inc.) and IL-6 (BMS603-2, Invitrogen; Thermo Fisher Scientific, Inc.) ELISA kits. A total of 50 μl serum samples were added to the prepared microwells of the plate and diluted twice with the sample solvent. To quantify the relative protein levels, standard solutions of various concentrations were added to additional wells instead of samples. To the resulting mixtures, 50 μl diluted biotin conjugate was added and the mixture was incubated for 2 h at room temperature. Subsequently, 100 μl streptavidin-HRP was added and incubated for 1 h at room temperature. The microwells were washed multiple times and stained with tetramethylbenzidine. The intensity of staining was assessed using an EFOS-9305 spectrophotometer (Shvabe Photosystems, Moscow, Russian Federation, https://www.shvabe.com) at a wavelength of 620 nm. The concentration of substances was calculated on the basis of a calibration curve constructed from the data of a titration of standard solutions. Detection of inflammatory cytokines was performed three times.

2.10. Statistical analysis

Statistical analysis was performed using Statistica 14.0 software (StatSoft, Moscow, Russia). The normality of the data was assessed using the Kolmogorov-Smirnov test. Non-parametric Kruskal-Wallis H-test was used for multiple comparisons. Mann-Whitney *U* test was used for comparisons between two independent groups. Data are presented as the mean ± standard error of the mean. $P < 0.05$ was considered to indicate a statistically significant difference.

3. Results

3.1. miR-204-5p expression is decreased in the lungs

First, it was investigated whether the miR-204-5p LNA inhibitor affects miRNA levels in tumor cells and in distant metastasis target organs: the lungs and liver. No changes were observed in the miRNA expression in melanoma tumor cells (Fig. 1, a), while a significant decrease in miR-204-5p expression was observed in the lungs of LNA-i-miR-204-5p-treated animals, compared with the Control and Negative Control groups (Fig. 1, b). In the liver tissue, no changes in miR-204-5p expression levels were observed in the LNA-i-miR-204-5p group as compared to the Control and Negative Control groups (Fig. 1, c).

Lungs are common site for metastatic development in the B16 melanoma model and one of the most common melanoma metastasis target organs in humans [22]. In the present study, it was further examined whether lung tissue undergoes a transformation during melanoma progression and miR-204-5 inhibition.

3.2. The number of CD45RO cells are decreased in LNA-i-miR-204-5p-transfected B16 melanoma-bearing mice

The lung, a target organ of melanoma metastasis, is characterized by a shift towards the pro-inflammatory phenotype, which corresponds to metastasis target organ rearrangement [23]. Therefore, lymphocytic infiltrate characterization was carried out and the presence of cancer-associated fibroblasts in the lungs was evaluated. Positivity of

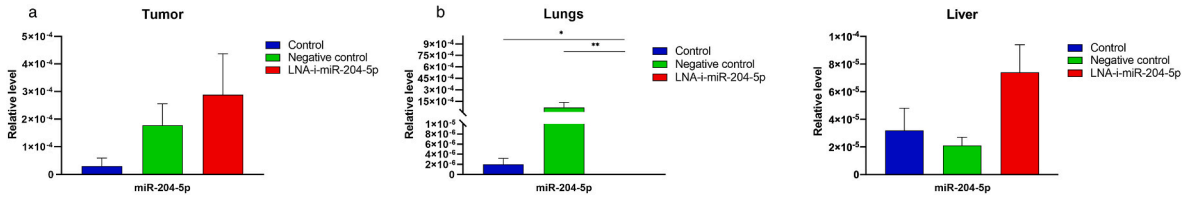

Fig. 1. Validation of the expression of miR-204-5p in melanoma tumor tissue and melanoma metastasis target organs (lungs and liver). (a) No changes were observed in the relative expression of miR-204-5p in the tumors of C57Bl6 B16 melanoma-bearing mice. (b) MiR-204-5p was downregulated in the lungs of the LNA-i-miR-204-5p group compared with the Negative Control, Control groups. (c) The level of miR-204-5p expression in the liver did not change significantly. *P < 0.05 in LNA-i-miR-204-5p versus Control; **P < 0.05 in LNA-i-miR-204-5p versus Negative Control.

cells for CD45RO, CD3, CD8, FOXP3 and α-SMA was evaluated, due to their presence in tumor microenvironment infiltrates [24]. According to the immunohistochemistry results, only CD45RO$^+$ cells were found to be decreased in the LNA-i-miR-204-5p group, by > 4-fold compared with the Control group and >10-fold compared with the Negative Control group (Fig. 2, a-f). A relatively small CD45RO$^+$ cell population was identified among the total number of cells in the lungs. Therefore, to confirm the possible effect of miR-204-5p on the number of CD45RO$^+$ cells, an attempt was made to reproduce the effect on PBMCs by transfecting them with a miR-204-5p inhibitor. Due to difficulty obtaining the required amount of mouse PBMCs, experiments were carried out in vitro using human leukocytes. Despite species differences between mice and humans, the regulation of miRNAs and their corresponding biological effects are conserved. The transfection efficacy was determined by evaluating the miR-204-5p expression using RT-qPCR, which was found to be decreased in the miR-204-5p inhibitor group compared to the Negative Control group (Fig. 3, f). No changes were observed in the apoptotic rate of the entire population of isolated PBMCs, whereas the number of Annexin$^+$/CD45RO$^+$ cells was found to be increased, as compared to the Negative Control (Fig. 3, a-e).

3.3. No toxic manifestations were observed in mice given LNA-i-miR-204-5p

Finally, it was determined whether the administration of miR-204-5p inhibitor had toxic effects on the treated animals. For this purpose, the weight and motor activity of animals were measured, internal organs were assessed using histopathological analysis and the organs were weighed. No loss in body weight was observed across the groups and animals of all three studied groups exhibited the same dynamics in terms of changes in body weight (Fig. 4, d). The activity index was decreased in the Negative Control and LNA-i-miR-204-5p groups compared with the Control group on days 9 and 10, whereas animals in the LNA-i-miR-204-5p group had a lower activity index compared with the control group on days 7–11 (Fig. 5, a). The mass of the liver, kidney, lung, heart, spleen and brain, as well as tumor mass and volume, were similar in all three groups (Fig. 4, a-c, Fig. 5, b).

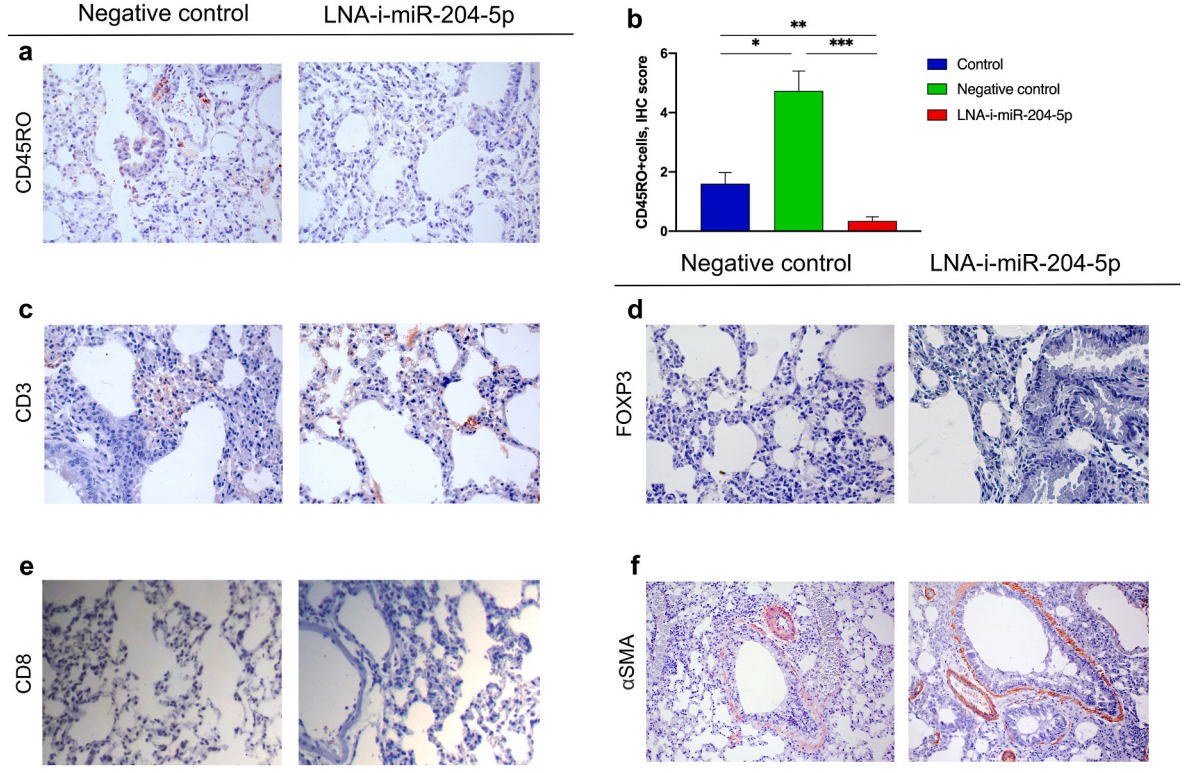

Fig. 2. Immunovisualization of lymphocytic infiltrates and α-SMA$^+$ cells in the lungs of C57Bl6 B16 melanoma-bearing mice. Immunostaining for (a) CD45RO$^+$, (c) CD3$^+$, (e) CD8$^+$, (d) FOXP3$^+$ and (f) α-SMA$^+$ cells in the Negative Control and LNA-i-miR-204-5p groups (magnification ×100). (b) Number of CD45RO-positive cells was decreased in the LNA-i-miR-204-5p compared with the Negative Control and Control groups. *P < 0.05 in Negative Control versus Control; **P < 0.001 in LNA-i-miR-204-5p versus Control; ***P < 0.001 in LNA-i-miR-204-5p versus Negative Control.

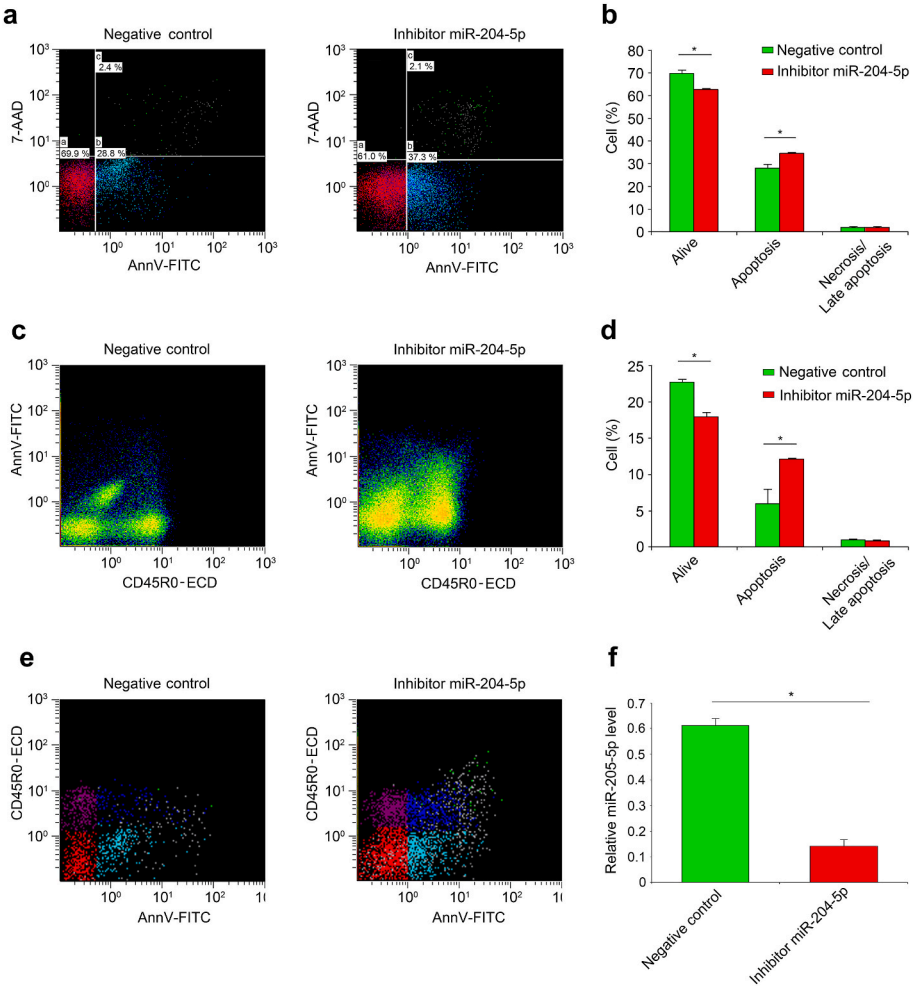

Fig. 3. Apoptosis and CD45RO expression in human PBMCs following transfection with the miR-204-5p inhibitor. A Dot plot diagrams of (a) Annexin V-FITC/7-AAD assay, (c) CD45RO, (e) Annexin V-FITC/CD45RO evaluation. (b) MiR-204-5p inhibitor transfection increased apoptosis in human PBMCs (*P < 0.05). (d) MiR-204-5p inhibitor transfection increased apoptosis in CD45RO$^+$ cells compared with Negative Control (*P < 0.05). (f) Decreased miR-204-5p relative expression in PBMCs following miR-204-5p inhibitor transfection (*P < 0.05). CD45RO apoptotic cells were defined as Annexin$^+$/CD45RO$^+$ cells.

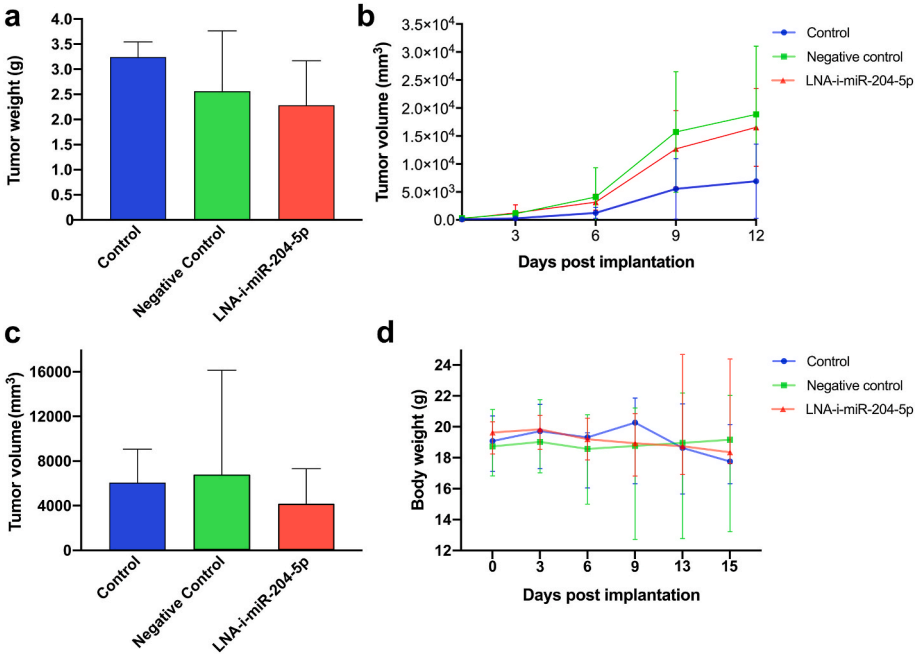

Fig. 4. C57Bl6 B16 melanoma-bearing mice treated with PBS (Control), Negative control a miRCURY LNA™ (Negative Control), and the mmu-miR-204-5p miRCURY LNA™ inhibitor (LNA-i-miR-204-5p). No changes in (a) tumor weight and (c) tumor volume at autopsy were observed within the three groups. No differences were found in the volumes of tumor nodes (b), as well as in the body weight of animals (d) recorded every three days during the experiment.

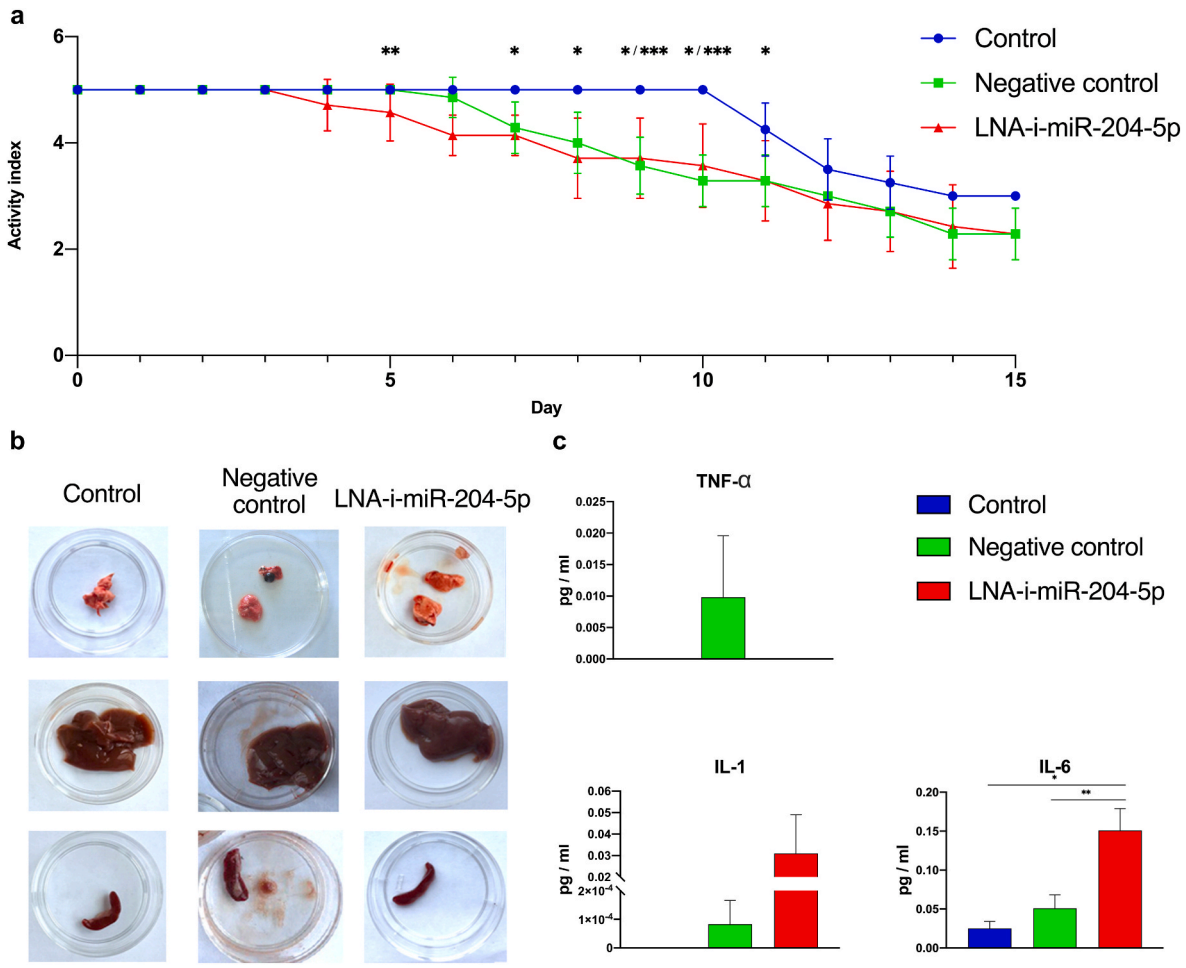

Fig. 5. Mice activity and plasma levels of the pro-inflammatory cytokines of C57Bl6 B16 melanoma-bearing mice following LNA-i-miR-204-5p transfection. (a) The activity index was decreased in the Negative Control and LNA-i-miR-204-5p groups compared with the Control group on days 9 and 10, whereas the LNA-i-miR-204-5p group exhibited a lower activity index compared with the Control group on days 7–11. (b) Image of the lungs, liver and spleen of animals in the Control, Negative Control and LNA-i-miR-204-5p group. Their mass, as well as the mass of the tumors, heart and brain, did not differ among the three studied groups. (c) The serum levels of tumor necrosis factor-α and IL-1 were not altered in the Control, Negative Control and LNA-i-miR-204-5p groups, whereas IL-6 levels were increased in the LNA-i-miR-204-5p compared with the Control and Negative Control. *P < 0.05 in LNA-i-miR-204-5p versus Control; **P < 0.05 in LNA-i-miR-204-5p versus Negative Control; ***P < 0.05 in Negative Control versus Control.

3.4. IL-6 plasma levels are elevated in LNA-i-miR-204-5p-transfected mice

Additionally, in the context of studying the toxicity of the use of the miR-204-5p LNA inhibitor in animals - TNF-α and IL-1 levels were not altered across the groups, whereas IL-6 was elevated in the LNA-i-miR-204-5p group, compared with the Control and Negative Control groups (Fig. 5, c).

4. Discussion

Since the first RNA interference-based [25] drug for hereditary amyloidosis treatment was approved, a new challenge has emerged in attempting to further develop RNA targeting and its application as a therapeutic tool. The tissue and disease specificity of miRNAs render them potential molecules for targeting various cancer types. Our previous studies revealed that miR-204-5p inhibitor application in vitro resulted in a decrease in the percentage of S-G2-phase^{+} cells, but promoted melanoma cell migration in vitro [13]. It was therefore examined whether the modulation of miR-204-5p levels in vivo affects melanoma growth and progression. B16 melanoma-bearing mice were systemically treated with an miR-204-5p-specific LNA inhibitor. First, it was determined whether the aforementioned inhibitor could reach tumor cells and cells in target organs of melanoma metastasis (lungs and liver). Indeed, miR-204-5p levels were found to be decreased in the lungs, but not in the tumor tissue. It is well established that blood supply to the tumors occurs through altered vasculature [26,27]. In addition, B16 melanoma cells are characterized by the phenomenon of vasculogenic mimicry in vivo [28], which potentiates drug resistance [29–31]. Poor penetration of LNA-i-miR-204-5p may also be due to its lower rate of diffusion to cancer cells, as a result of the relatively high interstitial fluid pressure [32]. Current research has focused on targeting oncogenic/onco-suppressive miRNAs for experimental cancer therapy. Previous studies have demonstrated the use of miR-155 targeting in xenograft mouse models containing lymphoma cell lines, where reduced miR-155 expression levels were associated with diminished tumor growth. Moreover, an miR-182 inhibitor was used in melanoma-bearing immunodeficient mice, and the dissemination of melanoma cells to distant organs was evaluated using in vivo imaging. The level of macrometastasis was reduced in the liver of *anti*-miR-182-treated animals, highlighting the pro-oncogenic and prometastatic role of miR-182 [33]. However, several limitations of miRNA-based therapy within clinical applications remain, including a lack of efficient delivery into the cells, pleiotropic functioning of miRNAs and rapid plasma degradation [34–36].

It was further investigated whether miR-204-5p induced changes in

pro-inflammatory cells in the lungs. Melanoma infiltration occurs through a polymorphic group of immune cells, mainly effector CD8 T cells, regulatory T cells and natural killer cells [37]. It is not well known how T cells participate in the reorganization of melanoma metastasis target organs due to tumor dissemination or premetastatic niche formation. Therefore, cytotoxic, memory and regulatory T cells, as well as α-SMA expression, which are linked to cancer-associated fibroblasts, were evaluated in the lungs of mice following treatment with LNA-i-miR-204-5p. No expression differences were observed in the $CD3^+$, $CD8^+$ and $FOXP3^+$ cells, whereas a prominent reduction was observed in the number of $CD45RO^+$ cells, which correspond to memory cells. CD45RO is an isoform of the common leucocyte antigen expressed on activated and memory T cells, as well as on B cells, monocytes, macrophages and granulocytes [38]. The CD45RO isoform of a receptor-type protein tyrosine phosphatase was shown to be able to translocate to lipid rafts resulting to the decrease of its soluble compartment on the cell membrane surface following IL-6 treatment, which was associated with changes in the CD45RO cell proliferation rate [39]. IL-12 was found to alter CD45RO distribution within rafts and the soluble fraction, thereby altering receptor-type protein tyrosine phosphatase accessibility to substrates, and modifying signaling and T cell activation [40]. The depletion of $CD45RO^+$ cells may be due to their apoptosis [41,42]. Therefore, the experiment was replicated in human PBMCs, and the results revealed that the number of $Annexin^+/CD45RO^-$ cells was increased following miR-204-5p inhibitor transfection, compared with the Negative Control group. Numerous studies have shown that miR-204-5p is involved in apoptosis [43,44]. MiR-204-5p inhibition has been shown to induce apoptosis in human B cells via endoplasmic reticulum stress proteins [45]. MiR-204-5p overexpression increased the sensitivity of neuroblastoma cells to chemotherapeutic agents cisplatin and etoposide by directly binding to its target genes, apoptosis-related BCL2 and neurotrophic receptor tyrosine kinase 2 [46]. In addition, miR-204-5p has been shown to bind to the CD5 mRNA isoform, which is predominant in unstimulated cells, thereby causing a delayed T cell activation and altered Fas-mediated apoptosis in T cells [47].

The findings of the present study revealed that IL-6 was increased in the serum of LNA-i-miR-204-5p-treated mice, which could be a result of the direct activation of macrophages by antisense oligonucleotides via toll-like receptors [48]. IL-6 alters T cell responses in the lung, including CD4 and CD8 T cell differentiation, and Th1 polarization [49]. The lack of any alterations in CD8 and $FOXP3^+$ cells in the lungs suggested that CD45RO alterations in lung tissue are more likely to be mediated by miR-204-5p expression alterations, rather than by the systemic effect of IL-6 elevation. However, IL-6 could affect mouse activity and lead to its decrease as well as a weight of mice [50–52].

Based on antisense oligonucleotide biodistribution [26], organs with the highest concentrations are the liver and kidneys. In the present study, it was shown that the modulation of miRNA expression occurred in the lungs. Lungs are often affected during the dissemination of various tumors, including melanoma. However, CD45RO cell depletion could affect the immune response and favor melanoma progression, which is consistent with previous studies reporting that miR-204-5p functions as a tumor suppressor [53,54]. The specific role of miR-204-5p in the regulation of leucocyte differentiation is yet to be fully elucidated. However, an immune-deficient mice model of breast cancer demonstrated increased expression levels of $CD4^+$ and $CD8^+$ in the tumor microenvironment following miR-204-5p overexpression, in addition to a higher level of $CD45^+$ cells in the tumor and spleen. These increased levels were a result of the direct activation of the PI3K/Akt signaling pathway by miR-204-5p [55]. Moreover, the effects of miR-204-5p in adipose-derived stem cell differentiation was revealed by targeting the PI3K/Akt signaling pathway [56]. Previous studies also demonstrated that miR-155 played a key role in determining the phenotype of tumor-infiltrating immune cells, as miR-155-knockout B16F10 melanoma mice exhibited an increased tumor burden compared with wild-type animals. Notably, miR-155 affected T-cell activation and interferon-ɤ production [57]. Furthermore, T-cell development was altered in CD45-knockout mice, as T-cells were less sensitive to apoptotic stimuli [58]. Therefore, additional studies are required to further clarify whether CD45RO downregulation mediated by the inhibitor LNA-i-miR-204-5p affects the antitumor immune response.

In conclusion, results of the present study demonstrated that the miR-204-5p LNA-specific inhibitor targets metastatic melanoma that has spread to distant organs, such as the lungs and liver. Treatment with LNA-i-miR-204-5p resulted in $CD45RO^+$ cell depletion in the lungs, consistent with the findings determined using in vitro miR-204-5p targeting in human blood mononuclear cells. Further investigations are required to clarify the specific role of miR-204-5p in immune cells, as selective targeting of miRNA expression levels may act as a novel approach for adjuvant chemotherapy.

Data availability

Not applicable.

Ethics approval

This study was performed in line with the principles of the Declaration of Helsinki and was approved by the Local Ethics Committee of the Krasnoyarsk State Medical University (approval no. 79/2017; date issued, November 22, 2017).

Consent to participate

Informed consent was obtained from all individual participants included in the study.

Consent to publish

No data needed a consent from participants is published.

Funding

The study was supported by a grant from the Russian Science Foundation (project N№19-15-00110П).

CRediT authorship contribution statement

Nadezhda Palkina: Conceptualization, Methodology, Formal analysis, Writing – original draft, Writing – review & editing. **Mariya Aksenenko:** Methodology, Investigation. **Danil Zemtsov:** Investigation, Validation. **Semyon Lavrentev:** Investigation, Validation. **Ivan Zinchenko:** Investigation, Validation. **Vasiliy Belenyuk:** Methodology, Investigation, Formal analysis. **Andrey Kirichenko:** Methodology, Formal analysis, Resources. **Andrey Savchenko:** Methodology, Formal analysis, Resources. **Tatiana Ruksha:** Conceptualization, Methodology, Resources, Supervision, Project administration, Writing – original draft, Writing – review & editing.

Declaration of competing interest

None.

References

[1] J. Larkin, V. Chiarion-Sileni, R. Gonzalez, J.J. Grob, P. Rutkowski, C.D. Lao, C. L. Cowey, D. Schadendorf, J. Wagstaff, R. Dummer, P.F. Ferrucci, M. Smylie, D. Hogg, A. Hill, I. Márquez-Rodas, J. Haanen, M. Guidoboni, M. Maio, P. Schöffski, M.S. Carlino, C. Lebbé, G. McArthur, P.A. Ascierto, G.A. Daniels, G. V. Long, L. Bastholt, J.I. Rizzo, A. Balogh, A. Moshyk, F.S. Hodi, J.D. Wolchok, Five-year survival with combined nivolumab and ipilimumab in advanced

melanoma, N. Engl. J. Med. 381 (2019) 1535–1546, https://doi.org/10.1056/NEJMoa1910836.
[2] R.W. Jenkins, D.E. Fisher, Treatment of advanced melanoma in 2020 and beyond, J. Invest. Dermatol. 20 (2020) 31257–31264, https://doi.org/10.1016/j.jid.2020.03.943.
[3] C. Robert, B. Karaszewska, J. Schachter, P. Rutkowski, A. Mackiewicz, D. Stroiakovski, B. Karaszewska, A. Hauschild, E. Levchenko, V. Chiarion Sileni, J. Schachter, C. Garbe, I. Bondarenko, H. Gogas, M. Mandalá, J.B.A.G. Haanen, C. Lebbé, A. Mackiewicz, P. Rutkowski, P.D. Nathan, A. Ribas, M.A. Davies, K. T. Flaherty, P. Burgess, M. Tan, E. Gasal, M. Voi, D. Schadendorf, G.V. Long, Five-year outcomes with dabrafenib plus trametinib in metastatic melanoma, N. Engl. J. Med. 381 (2019) 626–636, https://doi.org/10.1056/NEJMoa1904059.
[4] J. Massagué, K. Ganesh, Metastasis-initiating cells and ecosystems, Cancer Discov. 11 (2021) 971–994, https://doi.org/10.1158/2159-8290.CD-21-0010.
[5] N.M. Aiello, D.L. Bajor, R.J. Norgard, A. Sahmoud, N. Bhagwat, M.N. Pham, T. C. Cornish, C.A. Iacobuzio-Donahue, R.H. Vonderheide, B.Z. Stanger, Metastatic progression is associated with dynamic changes in the local microenvironment, Nat. Commun. 7 (2016) 12819–12827, https://doi.org/10.1038/ncomms12819.
[6] H. Zhang, T. Deng, R. Liu, M. Bai, L. Zhou, X. Wang, H. Yang, J. Li, T. Ning, D. Huang, H. Li, L. Zhang, G. Ying, Y. Ba, Exosome-delivered EGFR regulates liver microenvironment to promote gastric cancer liver metastasis, Nat. Commun. 8 (2017) 15016–15026, https://doi.org/10.1038/ncomms15016.
[7] T. Seimiya, M. Otsuka, T. Iwata, C. Shibata, E. Tanaka, T. Suzuki, K. Koike, Emerging roles of exosomal circular RNAs in cancer, Front. Cell Dev. Biol. 8 (2020), e568366, https://doi.org/10.3389/fcell.2020.568366.
[8] T. Ruksha, MicroRNA's control of cancer cell dormancy, Cell Div. 14 (2019) 11, https://doi.org/10.1186/s13008-019-0054-8.
[9] H. Zhang, Y. Li, M. Lai, The microRNA network and tumor metastasis, Oncogene 29 (2010) 937–948, https://doi.org/10.1038/onc.2009.406.
[10] J.M. Grixti, D. Ayers, P.J.R. Day, An analysis of mechanisms for cellular uptake of miRNAs to enhance drug delivery and efficacy in cancer chemoresistance, Noncoding RNA 7 (2021), e7020027, https://doi.org/10.3390/ncrna7020027.
[11] J. Elmén, M. Lindow, A. Silahtaroglu, M. Bak, M. Christensen, A. Lind-Thomsen, M. Hedtjärn, J.B. Hansen, H.F. Hansen, E.M. Straarup, K. McCullagh, P. Kearney, S. Kauppinen, Antagonism of microRNA-122 in mice by systemically administered LNA-antimiR leads to up-regulation of a large set of predicted target MRNAs in the liver, Nucleic Acids Res. 36 (2008) 1153–1162, https://doi.org/10.1093/nar/gkm1113.
[12] D. Adams, A. Gonzalez-Duarte, W.D. O'Riordan, C. Yang, M. Ueda, A.V. Kristen, I. Tournev, H.H. Schmidt, T. Coelho, J.L. Berk, K.P. Lin, G. Vita, S. Attarian, V. Planté-Bordeneuve, M.M. Mezei, J.M. Campistol, J. Buades, T.H. Brannagan, B. J. Kim, J. Oh, Y. Parman, Y. Sekijima, P.N. Hawkins, S.D. Solomon, M. Polydefkis, P.J. Dyck, P.J. Gandhi, S. Goyal, J. Chen, A.L. Strahs, S.V. Nochur, M.T. Sweetser, P.P. Garg, A.K. Vaishnaw, J.A. Gollob, O.B. Suhr, Patisiran, an RNAi therapeutic, for hereditary transthyretin amyloidosis, N. Engl. J. Med. 379 (2018) 11–21, https://doi.org/10.1056/NEJMoa1716153.
[13] N. Palkina, A. Komina, M. Aksenenko, A. Moshev, A. Savchenko, T. Ruksha, miR-204-5p and miR-3065-5p exert antitumor effects on melanoma cells, Oncol. Lett. 15 (2018) 8269–8280, https://doi.org/10.3892/ol.2018.8443.
[14] B.S. Hong, H.S. Ryu, N. Kim, J. Kim, E. Lee, H. Moon, K.H. Kim, M.S. Jin, N. H. Kwon, S. Kim, D. Kim, D.H. Chung, K. Jeong, K. Kim, K.Y. Kim, H.B. Lee, W. Han, J. Yun, J.I. Kim, D.Y. Noh, H.G. Moon, Tumor suppressor miRNA-204-5p regulates growth, metastasis, and immune microenvironment remodeling in breast cancer, Cancer Res. 79 (2019) 1520–1534, https://doi.org/10.1158/0008-5472.CAN-18-0891.
[15] H. Toda, S. Kurozumi, Y. Kijima, T. Idichi, Y. Shinden, Y. Yamada, Molecular pathogenesis of triple-negative breast cancer based on microRNA expression signatures: antitumor miR-204-5p targets AP1S3, J. Hum. Genet. 63 (2018) 1197–1210, https://doi.org/10.1038/s10038-018-0510-3.
[16] C.Y. Ooi, D.R. Carter, B. Liu, C. Mayoh, A. Beckers, A. Lalwani, Network modeling of microRNA-mRNA interactions in neuroblastoma tumorigenesis identifies miR-204 as a direct inhibitor of MYCN, Cancer Res. 78 (2018) 3122–3134, https://doi.org/10.1158/0008-5472.CAN-17-3034.
[17] M. Vitiello, A. Tuccoli, R. D'Aurizio, S. Sarti, L. Giannecchini, S. Lubrano, A. Marranci, M. Evangelista, S. Peppicelli, C. Ippolito, I. Barravecchia, E. Guzzolino, V. Montagnani, M. Gowen, E. Mercoledi, A. Mercatanti, L. Comelli, S. Gurrieri, L.W. Wu, O. Ope, K. Flaherty, G.M. Boland, M.R. Hammond, L. Kwong, M. Chiariello, B. Stecca, G. Zhang, A. Salvetti, D. Angeloni, L. Pitto, L. Calorini, G. Chiorino, M. Pellegrini, M. Herlyn, I. Osman, L. Poliseno, Context-dependent miR-204 and miR-211 affect the biological properties of amelanotic and melanotic melanoma cells, Oncotarget 8 (2017) 25395–25417, https://doi.org/10.18632/oncotarget.15915.
[18] S. Sarti, R. De Paolo, C. Ippolito, A. Pucci, L. Pitto, L. Poliseno, Inducible modulation of miR-204 levels in a zebrafish melanoma model, Biol Open 9 (2020), ebio053785, https://doi.org/10.1242/bio.053785.
[19] N. Palkina, A. Tyumentseva, M. Aksenenko, R. Belonogov, S. Lavrentev, T. Ruksha, Toxicity of miR-204-5p inhibition for melanoma B16 cells in vitro and mice in vivo, Cell and Tissue Biology 12 (2018) 307–314, https://doi.org/10.1134/S1990519X18040077.
[20] A. Kalinina, I. Golubeva, I. Kudryavtsev, N. Khromova, E. Antoshina, L. Trukhanova, T. Gorkova, D. Kazansky, L. Khromykh, Cyclophilin A is a factor of antitumor defense in the early stages of tumor development, Int. Immunopharm. 94 (2021), 107470, https://doi.org/10.1016/j.intimp.2021.107470.
[21] A. Komina, N. Palkina, M. Aksenenko, S. Tsyrenzhapova, T. Ruksha, Antiproliferative and pro-apoptotic effects of miR-4286 inhibition in melanoma cells, PLoS One 11 (2016), e0168229, https://doi.org/10.1371/journal.pone.0168229.
[22] R. Giavazzi, A. Decio, Syngeneic murine metastasis models: B16 melanoma, Methods Mol. Biol. 1070 (2014) 131–140, https://doi.org/10.1007/978-1-4614-8244-4_10.
[23] M. Han, J. Xu, Y. Bi, M. Jiang, X. Xu, Q. Liu, Q. Liu, J. Jia, Primary tumor regulates the pulmonary microenvironment in melanoma carcinoma model and facilitates lung metastasis, J. Cancer Res. Clin. Oncol. 139 (2013) 57–65, https://doi.org/10.1007/s00432-012-1299-7.
[24] G. Garcia-Vicién, A. Mezheyeuski, M. Bañuls, N. Ruiz-Roig, D.G. Molleví, The tumor microenvironment in liver metastases from colorectal carcinoma in the context of the histologic growth patterns, Int. J. Mol. Sci. 22 (2021) e1544, https://doi.org/10.3390/ijms22041544.
[25] H. Ledford, Gene-silencing technology gets first drug approval after 20-year wait, Nature 560 (2018) 291–292, https://doi.org/10.1038/d41586-018-05867-7.
[26] P.J. White, F. Anastasopoulos, C.W. Pouton, B.J. Boyd, Overcoming biological barriers to in vivo efficacy of antisense oligonucleotides, Mol. Med. 11 (2009) e10, https://doi.org/10.1017/S1462399409001021.
[27] S. Nishide, J. Uchida, S. Matsunaga, K. Tokudome, T. Yamaguchi, K. Kabei, T. Moriya, K. Miura, T. Nakatani, S. Tomita, Prolyl-hydroxylase inhibitors reconstitute tumor blood vessels in mice, J. Pharmacol. Sci. 143 (2020) 122–126, https://doi.org/10.1016/j.jphs.2020.02.010.
[28] S.W. Zhang, D.F. Zhang, B.C. Sun, Vasculogenic mimicry: current status and future prospects, Cancer Lett. 254 (2007) 157–164, https://doi.org/10.1016/j.canlet.2006.12.036.
[29] M.A. Andonegui-Elguera, Y. Alfaro-Mora, R. Cáceres-Gutiérrez, C.H.S. Caro-Sánchez, L.A. Herrera, J. Díaz-Chávez, An overview of vasculogenic mimicry in breast cancer, Front. Oncol. 10 (2020), e220, https://doi.org/10.3389/fonc.2020.00220.
[30] A. Vartanian, M. Baryshnikova, O. Burova, D. Afanasyeva, V. Misyurin, A. Belyavsky, Z. Shprakh, Inhibitor of vasculogenic mimicry restores sensitivity of resistant melanoma cells to DNA-damaging agents, Melanoma Res. 27 (2017) 8–16, https://doi.org/10.1097/cmr.0000000000000308.
[31] C. Lezcano, C.-W. Lee, A.R. Larson, A.M. Menzies, R.F. Kefford, J.F. Thompson, M. C. Mihm Jr., S. Ogino, G.V. Long, R.A. Scolyer, G.F. Murphy, Evaluation of stromal HGF immunoreactivity as a biomarker for melanoma response to RAF inhibitors, Mod. Pathol. 27 (2014), 11931202, https://doi.org/10.1038/modpathol.2013.226.
[32] C. Li, L. Li, A.C. Keates, Targeting cancer gene therapy with magnetic nanoparticles, Oncotarget 3 (2012) 365–370, https://doi.org/10.18632/oncotarget.490.
[33] C. Huynh, M.F. Segura, A. Gaziel-Sovran, S. Menendez, F. Darvishian, L. Chiriboga, B. Levin, D. Meruelo, I. Osman, J. Zavadil, E.G. Marcusson, E. Hernando, Efficient in vivo microRNA targeting of liver metastasis, Oncogene 30 (2011) 1481–1488, https://doi.org/10.1038/onc.2010.523.
[34] M. Perepelyuk, C. Maher, A. Lakshmikuttyamma, S.A. Shoyele, Aptamer-hybrid nanoparticle bioconjugate efficiently delivers miRNA-29b to non-small-cell lung cancer cells and inhibits growth by downregulating essential oncoproteins, Int. J. Nanomed. 11 (2016) 3533–3544, https://doi.org/10.2147/IJN.S110488.
[35] B. Montico, G. Giurato, G. Pecoraro, A. Salvati, A. Covre, F. Colizzi, A. Steffan, A. Weisz, M. Maio, L. Sigalotti, E. Fratta, The pleiotropic role of circular and long noncoding RNAs in cutaneous melanoma, Mol Oncol 16 (2021) 565–593, https://doi.org/10.1002/1878-0261.13034.
[36] A.K. Chaudhary, G. Mondal, V. Kumar, K. Kattel, R.I. Mahato, Chemosensitization and inhibition of pancreatic cancer stem cell proliferation by overexpression of microRNA-205, Cancer Lett. 402 (2017) 1–8, https://doi.org/10.1016/j.canlet.2017.05.007.
[37] M. Antohe, R.I. Nedelcu, L. Nichita, C.G. Popp, M. Cioplea, A. Brinzea, A. Hodorogea, A. Calinescu, M. Balaban, D.A. Ion, C. Diaconu, C. Bleotu, D. Pirici, S.A. Zurac, G. Turcu, Tumor infiltrating lymphocytes: the regulator of melanoma evolution, Oncol. Lett. 17 (2019) 4155–4161, https://doi.org/10.3892/ol.2019.9940.
[38] C.-L. Yu, H.-S. Yu, K.-H. Sun, S.-C. Hsieh, C.-Y. Tsai, Anti-CD45 isoform antibodies enhance phagocytosis and gene expression of IL-8 and TNF-alpha in human neutrophils by differential suppression on protein tyrosine phosphorylation and p56lck tyrosine kinase, Clin. Exp. Immunol. 129 (2002) 78–85, https://doi.org/10.1046/j.1365-2249.2002.01907.x.
[39] F.J. Li, N. Tsuyama, H. Ishikawa, M. Obata, S. Abroun, S. Liu, K. Otsuyama, X. Zheng, Z. Ma, Y. Maki, M.M. Kawano, A rapid translocation of CD45RO but not CD45RA to lipid rafts in IL-6-induced proliferation in myeloma, Blood 105 (2005) 3295–3302, https://doi.org/10.1182/blood-2004-10-4083.
[40] J. Salgado, J. Lojo, J.L. Alonso-Lebrero, C. Lluis, R. Franco, O.J. Cordero, M. Nogueira, A role for interleukin-12 in the regulation of T cell plasma membrane compartmentation, J. Biol. Chem. 278 (2003) 24849–24857, https://doi.org/10.1074/jbc.M212978200.
[41] S.A. Trushin, G.D. Bren, A.D. Badley, CD4 T cells treated with gp120 acquire a CD45R0+/CD45RA+ phenotype, Open Virol. J. 3 (2009) 21–25, https://doi.org/10.2174/1874357900903010021.
[42] S.J. Klaus, S.P. Sidorenko, E.A. Clark, CD45 ligation induces programmed cell death in T and B lymphocytes, J. Immunol. 156 (1996) 2743–2753.
[43] I. Conte, K.D. Hadfield, S. Barbato, S. Carrella, M. Pizzo, R.S. Bhat, A. Carissimo, M. Karali, L.F. Porter, J. Urquhart, S. Hateley, J. O'Sullivan, F.D. Manson, S. C. Neuhauss, S. Banfi, G.C. Black, MiR-204 is responsible for inherited retinal dystrophy associated with ocular coloboma, Proc. Natl. Acad. Sci. U.S.A. 112 (2015) 3236–3245, https://doi.org/10.1073/pnas.1401464112.

[44] Y. Kuwano, K. Nishida, K. Kajita, Y. Satake, Y. Akaike, K. Fujita, S. Kano, K. Masuda, K. Rokutan, Transformer 2 beta and miR-204 regulate apoptosis through competitive binding to 3' UTR of BCL2 mRNA, Cell Death Differ. 22 (2015) 815–825, https://doi.org/10.1038/cdd.2014.176.
[45] F.A. Grieco, A.A. Schiavo, F. Brozzi, J. Juan-Mateu, M. Bugliani, P. Marchetti, D. L. Eizirik, The miRNAs miR-211-5p and miR-204-5p modulate ER stress in human beta cells, J. Mol. Endocrinol. 63 (2019) 139–149, https://doi.org/10.1530/JME-19-0066.
[46] J. Ryan, A. Tivnan, J. Fay, K. Bryan, M. Meehan, L. Creevey, J. Lynch, I.M. Bray, A. O'Meara, A.M. Davidoff, MicroRNA-204 increases sensitivity of neuroblastoma cells to cisplatin and is associated with a favorable clinical outcome, Br. J. Cancer 107 (2012) 967–976, https://doi.org/10.1038/bjc.2012.356.
[47] R.G. Domingues, I. Lago-Baldaia, I. Pereira-Castro, J.M. Fachini, L. Oliveira, D. Drpic, N. Lopes, T. Henriques, J.R. Neilson, A.M. Carmo, A. Moreira, CD5 expression is regulated during human T-cell activation by alternative polyadenylation, PTBP1, and miR-204, Eur. J. Immunol. 46 (2016) 1490–1503, https://doi.org/10.1002/eji.201545663.
[48] S. Agrawal, The evolution of antisense oligonucleotide chemistry-a personal journey, Biomedicines 9 (2021) 503–517, https://doi.org/10.3390/biomedicines9050503.
[49] W. Wu, K.K. Dietze, K. Gibbert, K.S. Lang, M. Trilling, H. Yan, J. Wu, D. Yang, M. Lu, M. Roggendorf, U. Dittmer, J. Liu, TLR ligand induced IL-6 counter-regulates the anti-viral CD8+T cell response during an acute retrovirus infection, Sci. Rep. 5 (2015), 10501, https://doi.org/10.1038/srep10501.
[50] A. Aniszewska, J. Szymanski, M.M. Winnicka, K. Turlejski, Interleukin 6 deficiency affects spontaneous activity of mice in age- and sex-dependent manner, Acta Neurobiol. Exp. 74 (2014) 424–432.
[51] M. Erta, M. Giralt, F.L. Esposito, O. Fernandez-Gayol, J. Hidalgo, Astrocytic IL-6 mediates locomotor activity, exploration, anxiety, learning and social behavior, Horm. Behav. 73 (2015) 64–74. https://doi.org/10.1016/j.yhbeh.2015.06.016.
[52] O. Patsalos, B. Dalton, H. Himmerich, Effects of IL-6 signaling pathway inhibition on weight and BMI: a systematic review and meta-analysis, Int. J. Mol. Sci. 21 (2020) 6290, https://doi.org/10.3390/ijms21176290.
[53] M. Galasso, C. Morrison, L. Minotti, F. Corrà, C. Zerbinati, C. Agnoletto, Loss of miR-204 expression is a key event in melanoma, Mol. Cancer 17 (2018) e75, https://doi.org/10.1186/s12943-018-0819-8.
[54] A. Toll, R. Salgado, B. Espinet, A. Díaz-Lagares, E. Hernández-Ruiz, E. Andrades, MiR-204 silencing in intraepithelial to invasive cutaneous squamous cell carcinoma progression, Mol. Cancer 15 (2016) e53, https://doi.org/10.1186/s12943-016-0537-z.
[55] S. Hong, H.S. Ryu, N. Kim, J. Kim, E. Lee, H. Moon, K.H. Kim, M.S. Jin, N.H. Kwon, S. Kim, D. Kim, D.H. Chung, K. Jeong, K. Kim, K.Y. Kim, H.B. Lee, W. Han, J. Yun, J.I. Kim, D.Y. Noh, H.G. Moon, Tumor suppressor miRNA-204-5p regulates growth, metastasis, and immune microenvironment remodeling in breast cancer, Cancer Res. 79 (2019) 1520–1534, https://doi.org/10.1158/0008-5472.CAN-18-0891.
[56] X. Liu, Z. Li, H. Liu, Y. Zhu, D. Xia, S. Wang, R. Gu, P. Zhang, Y. Liu, Y. Zhou, Flufenamic acid inhibits adipogenic differentiation of mesenchymal stem cells by antagonizing the PI3K/AKT signaling pathway, Stem Cell. Int. 16 (2020), 1540905, https://doi.org/10.1155/2020/1540905.
[57] H.A. Ekiz, T.B. Huffaker, A.H. Grossmann, W.Z. Stephens, M.A. Williams, J. L. Round, R.M. O'Connell, MicroRNA-155 coordinates the immunological landscape within murine melanoma and correlates with immunity in human cancers, JCI Insight 4 (2019), e126543, https://doi.org/10.1172/jci.insight.126543.
[58] K.F. Byth, L.A. Conroy, S. Howlett, A.J. Smith, J. May, D.R. Alexander, N. Holmes, CD45-null transgenic mice reveal a positive regulatory role for CD45 in early thymocyte development, in the selection of CD4+CD8+ thymocytes, and B cell maturation, J. Exp. Med. 183 (1996) 1707–1718, https://doi.org/10.1084/jem.183.4.1707.